Supporting Information

Multi-heterostructure with multi-interface for efficient hydrogen evolution reaction towards industrial alkaline seawater

Kai Zhang,[a] Qingmei Su,[*b] Yvjie Lv,[a] Weihao Shi,[a] Pinpin Wang,[e] Zhiyong Wang,[b,d] Wenqi Zhao,[b] Miao Zhang,[b] Shukai Ding,[b] Shufang Ma,[b] Gaohui Du,[*b] and Bingshe Xu[b,c]

[a] School of Materials Science & Engineering, Shaanxi University of Science and Technology, Xi'an, 710021, P. R. China.

[b] Materials Institute of Atomic and Molecular Science, School of Physics & Information Science, Shaanxi University of Science and Technology, Xi'an, 710021, P. R. China.

[c] Key Laboratory of Interface Science and Engineering in Advanced Materials, Taiyuan University of Technology, Taiyuan, 030024, P. R. China

[d] Beijing University of Technology, Chaoyang District, Beijing, 100124, P. R. China

[e] College of Food Science and Pharmaceutical Engineering, Zaozhuang University, Zaozhuang, 277160, P. R. China

Corresponding authors:

E-mail addresses: suqingmei@sust.edu.cn (Q. Su), dugaohui@sust.edu.cn (G. Du)

Supporting Figures

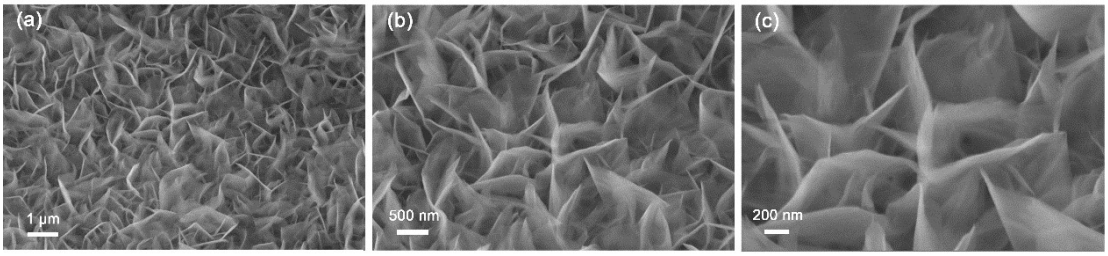

Figure S1. The SEM images of $NiCo_2O_4$ nanosheet arrays on the Ni foam.

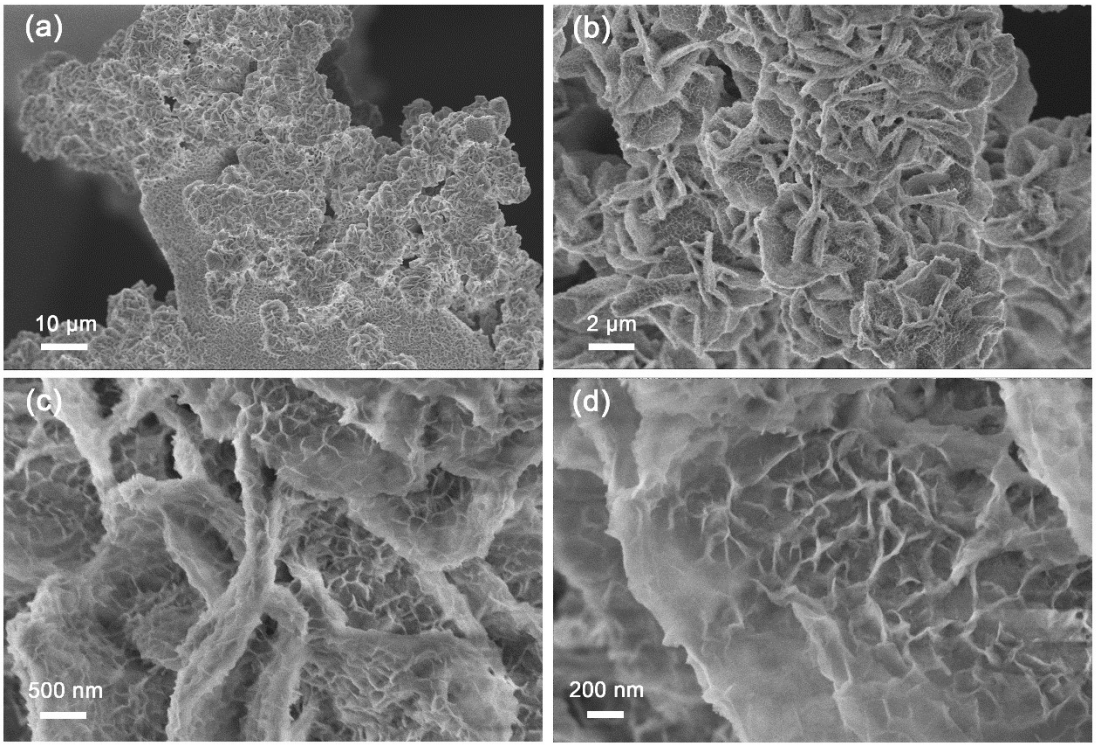

Figure S2. The SEM images of the $NiCo_2O_4$@$NiMoO_4$ on the Ni foam.

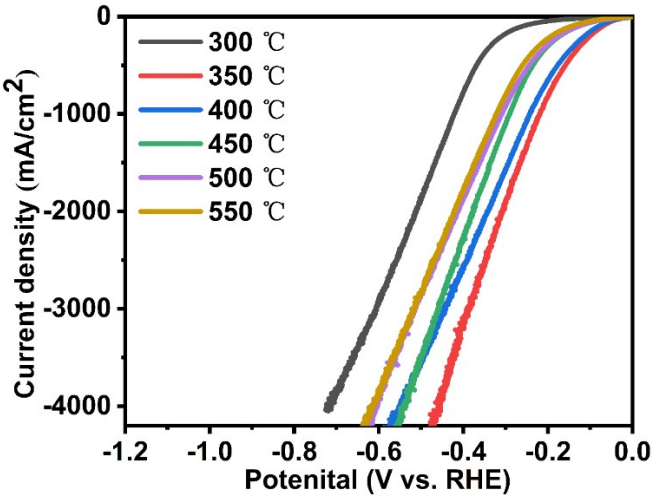

Figure S3. The LSV polarization curves with 90% iR compensation of the H_2-$NiCo_2O_4$@$NiMoO_4$ nanosheets calcined at different reduction temperatures under H_2/Ar atmosphere in 1.0 M KOH solution.

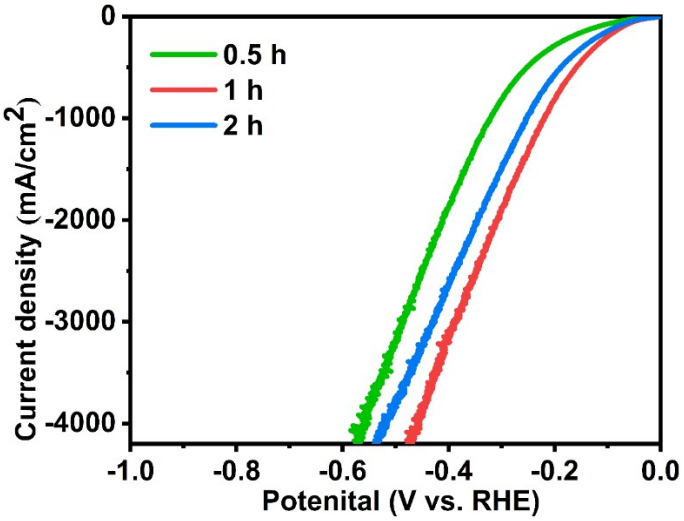

Figure S4. The LSV polarization curves with 90% iR compensation of the H_2-$NiCo_2O_4$@$NiMoO_4$ nanosheets calcined at 350 ℃ for different reduction times under H_2/Ar atmosphere in 1.0 M KOH solution.

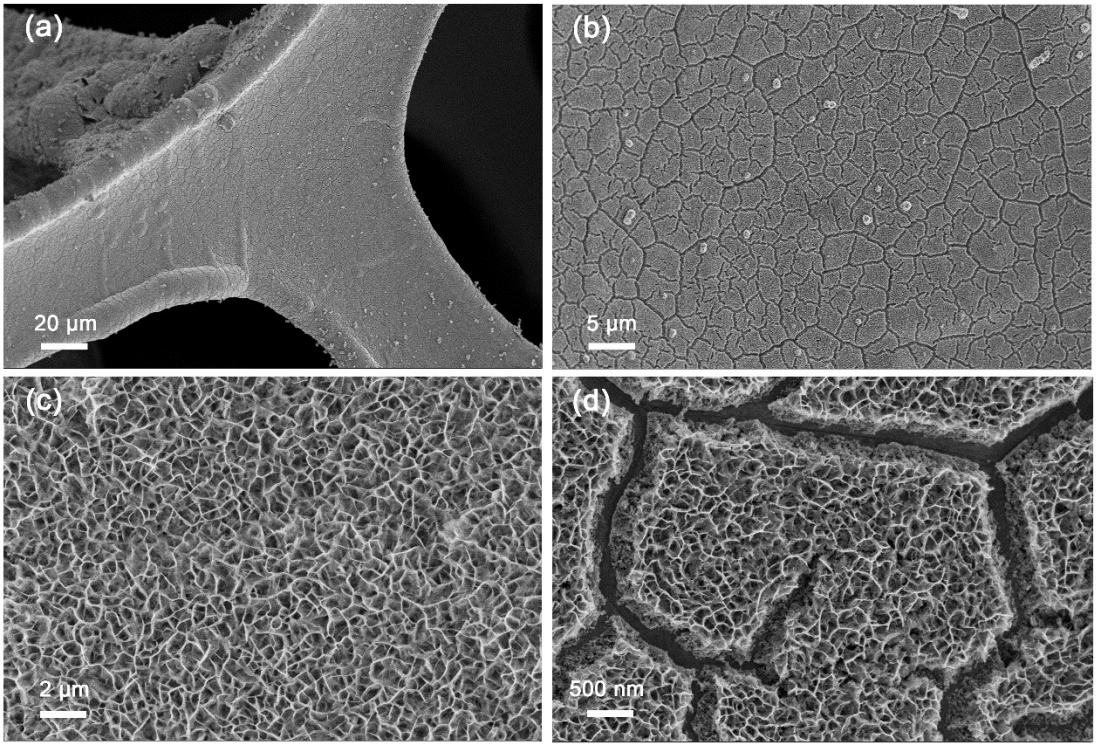

Figure S5. The SEM images of H_2-$NiMoO_4$ nanosheet arrays on the Ni foam.

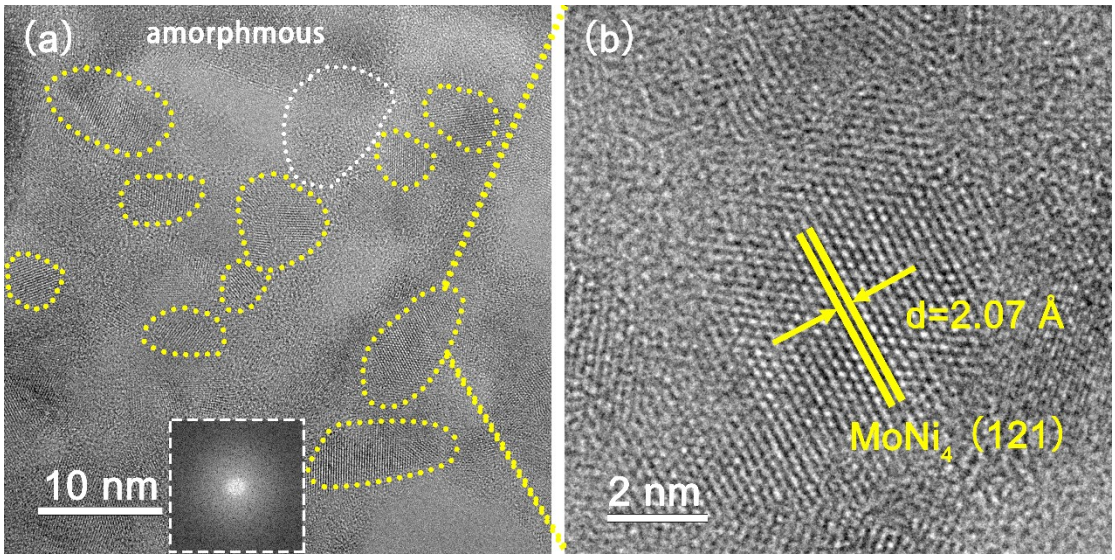

Figure S6. (a) The HRTEM image of the H_2-$NiMoO_4$ nanosheet arrays; (b) the enlarge picture of (a).

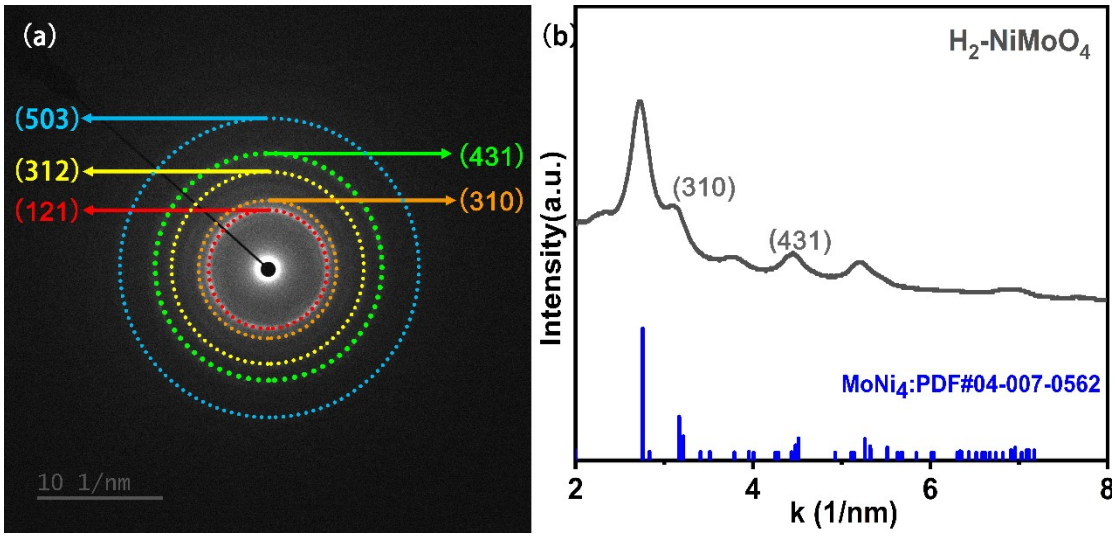

Figure S7. Radially integrated intensity of the diffraction patterns for H_2-$NiMoO_4$.

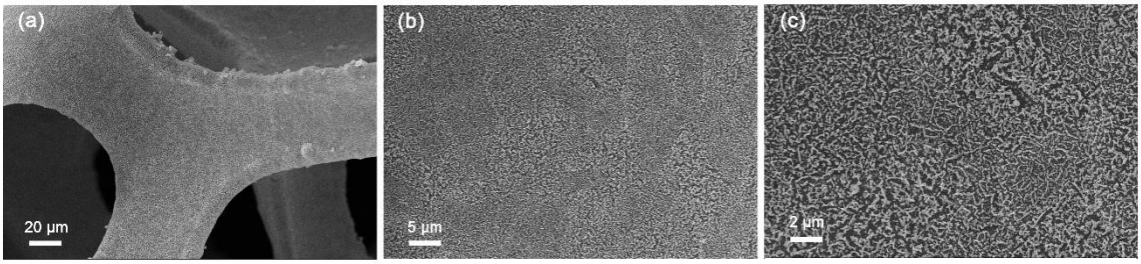

Figure S8. The SEM images of H_2-$NiCo_2O_4$ on Ni foam.

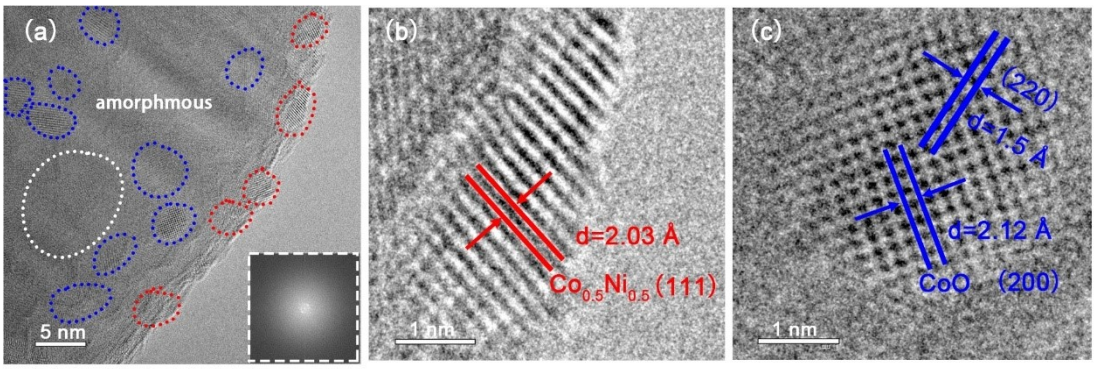

Figure S9. (a) The TEM image of H_2-$NiCo_2O_4$; (b-d) the enlarge pictures of (a).

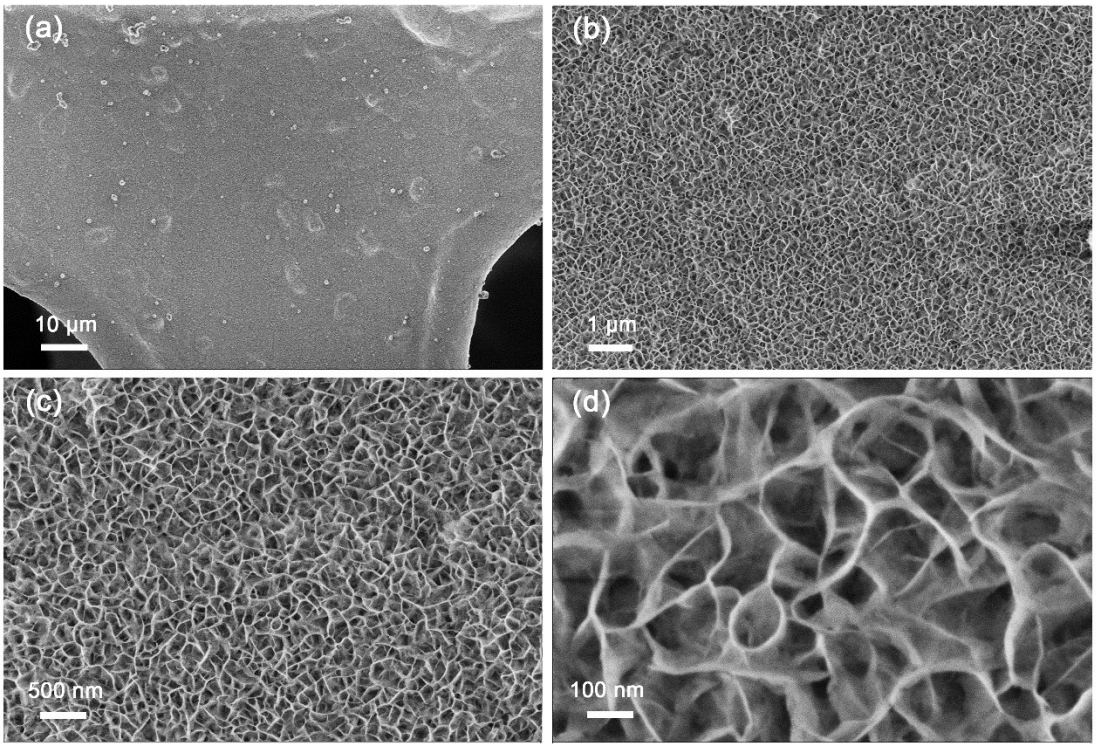

Figure S10. The SEM images of the $NiMoO_4$ nanosheet arrays on the Ni foam.

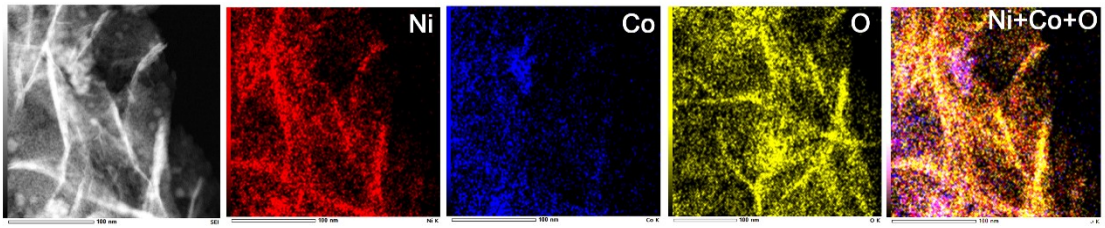

Figure S11. The HAADF-STEM image of H_2-$NiCo_2O_4$@$NiMoO_4$ and the corresponding energy-dispersive X-ray spectroscopy (EDS) elemental dispersion mappings for Ni, Co and Mo.

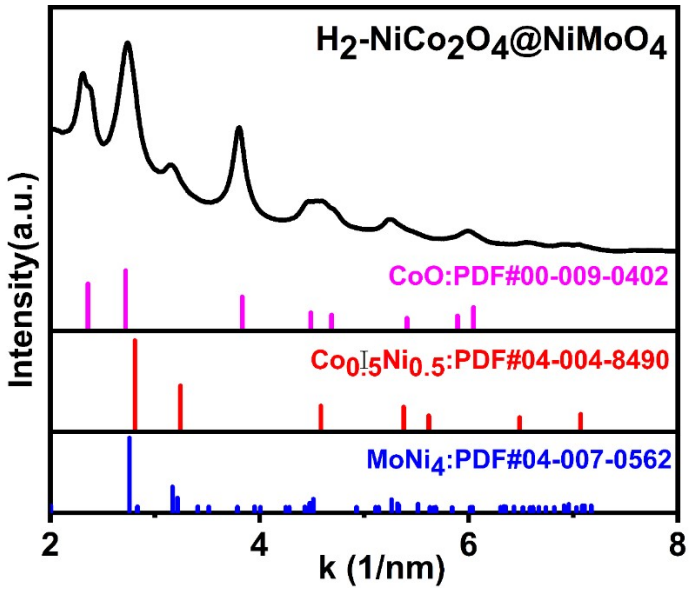

Figure S12. Radially integrated intensity of the diffraction patterns.

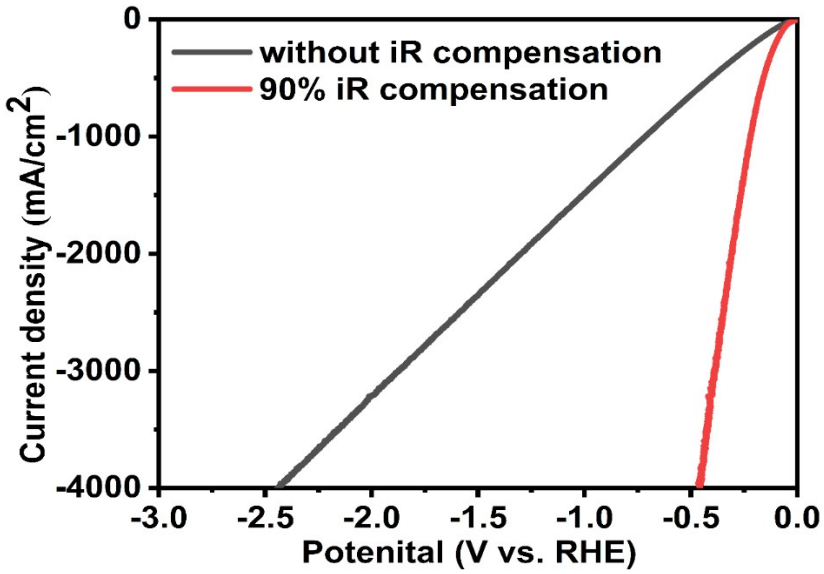

Figure S13. The polarization curves of H_2-$NiCo_2O_4$@$NiMoO_4$ (1 M KOH) for HER without and with 90% iR compensation, where the electrolyte resistance (R) is approximately 1.75 Ω.

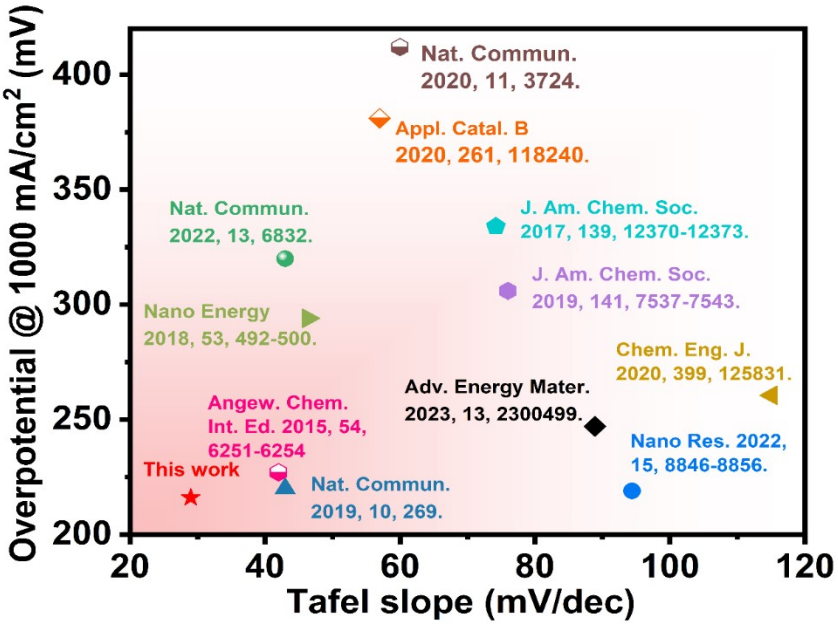

Figure S14. The comparative overpotentials of reported electrocatalysts for HER at 1000 mA/cm^2 in 1 M KOH electrolyte.

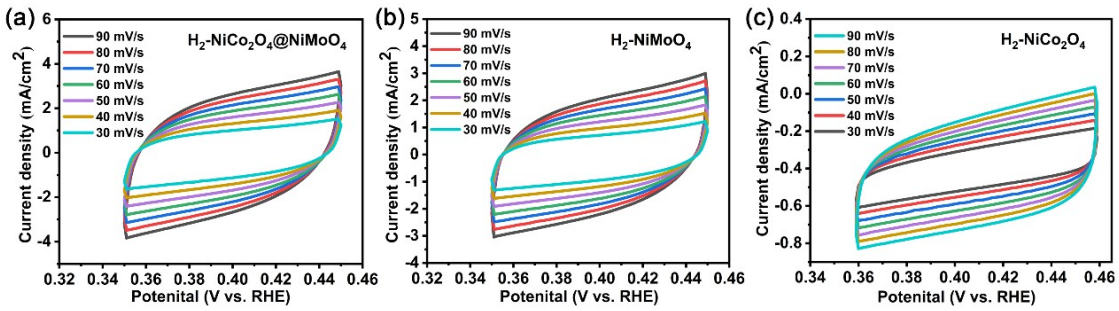

Figure S15. (a-c) Cyclic voltammetry curves at various scan rates of H_2-$NiCo_2O_4$@$NiMoO_4$, H_2-$NiMoO_4$ and H_2-$NiCo_2O_4$ in 1.0 M KOH solution, respectively.

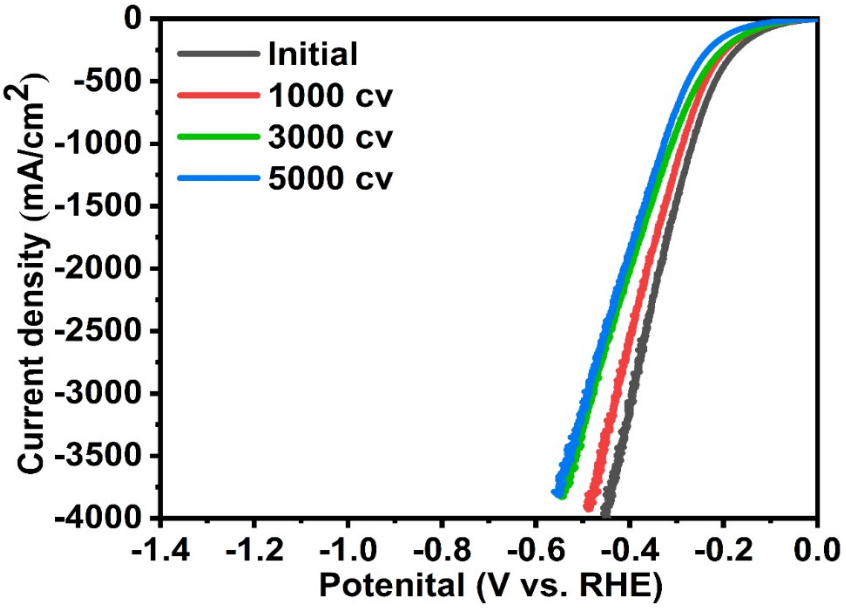

Figure S16. The CV stability tests of H_2-$NiCo_2O_4$@$NiMoO_4$ initial and after 1000, 3000, 5000 cycles in 1.0 M KOH solution.

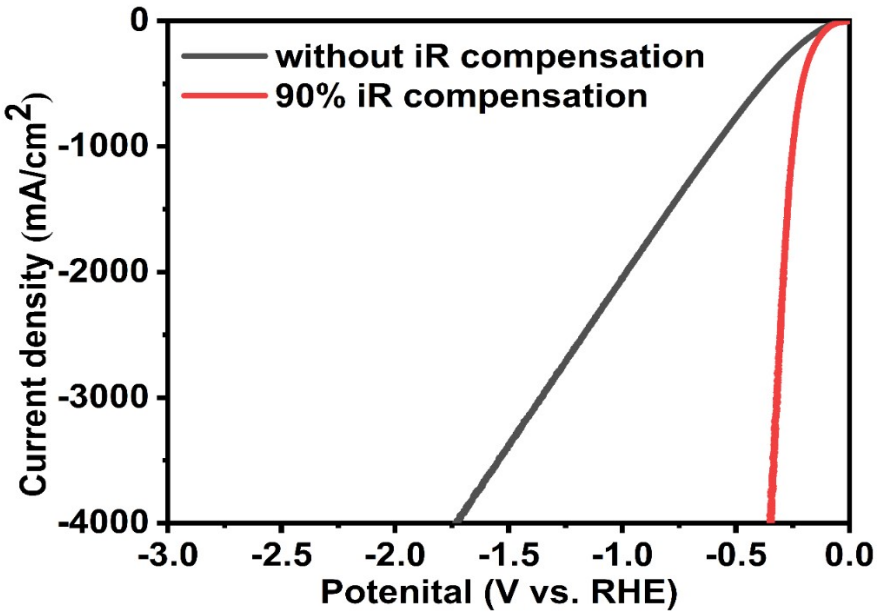

Figure S17. The polarization curves of H_2-$NiCo_2O_4$@$NiMoO_4$ (1 M KOH seawater) for HER without and with 90% iR compensation.

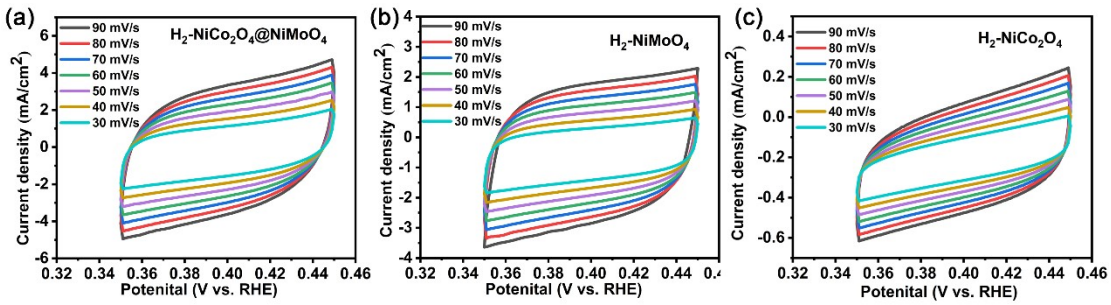

Figure S18. (a-c) Cyclic voltammetry curves of H_2-$NiCo_2O_4$@$NiMoO_4$, H_2-@$NiMoO_4$ and H_2-$NiCo_2O_4$ in 1.0 M KOH seawater, respectively.

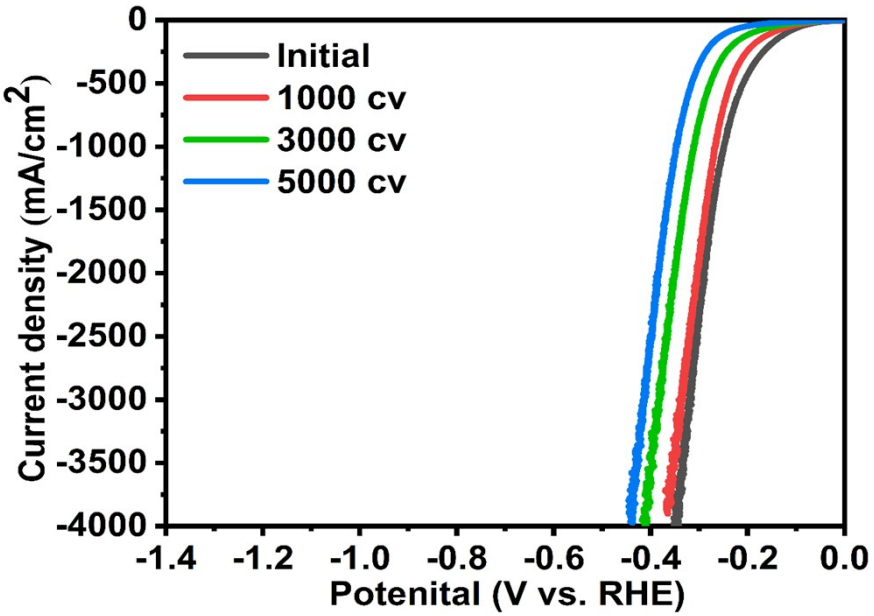

Figure S19. The CV stability tests of H_2-$NiCo_2O_4$@$NiMoO_4$ initial and after 1000, 3000, 5000 cycles.

Table S1. The HER performance comparisons of the H_2-$NiCo_2O_4$@$NiMoO_4$ with reported electrocatalysts.

Electrocatalyst	Electrolyte	Overpotential at 1000 mA/cm^2	Tafel slope	Reference
MoNi@NF	1 M KOH	219 mV	94.5 mV/dec	[1]
MoS_2/Mo_2C	1 M KOH	220 mV	43 mV/dec	[2]
Co-P	1 M KOH	227 mV	42 mV/dec	[3]
NiCoP-120	1 M KOH	247 mV	88.9 mV/dec	[4]
F-Co_2P/Fe_2P/IF	1 M KOH	260.5 mV	115.01 mV/dec	[5]
$Ni_{2(1-x)}Mo_{2x}P$	1 M KOH	294 mV	46.4 mV/dec	[6]
Ni_2P/NF	1 M KOH	306 mV	76 mV/dec	[7]
$CuMo_6S_8$/Cu	1 M KOH	320 mV	43 mV/dec	[8]
α-MoB_2	1 M KOH	334 mV	74.2 mV/dec	[9]
A-NiCo LDH/NF	1 M KOH	381 mV	57 mV/dec	[10]
HC-MoS_2/Mo_2C	1 M KOH	412 mV	60 mV/dec	[11]
H_2-$NiCo_2O_4$@$NiMoO_4$	1 M KOH	216 mV	29 mV/dec	This work

References

1 L. Guo, Q. Yu, X. Zhai and J. Chi, *nano Res.*, 2022, **15**, 8846–8856.

2 Y. Luo, L. Tang, U. Khan, Q. Yu, H. Cheng, X. Zou and B. Liu, *Nat. Commun.*, 2019, **10**, 269.

3 N. Jiang, B. You, M. Sheng and Y. Sun, *Angew. Chemie Int. Ed.*, 2015, **54**, 6251–6254.

4 D. Chen, H. Bai, J. Zhu, C. Wu, H. Zhao, D. Wu, J. Jiao, P. Ji and S. Mu, *Adv. Energy Mater.*, 2023, **13**, 2300499.

5 X. Zhang, Y. Zhu, Y. Chen, S. Dou, X. Chen, B. Dong and B. Guo, *Chem. Eng. J.*, 2020, **399**, 125831.

6 L. Yu, I. Kumar, Y. Xie, H. Zhou and J. Sun, *Nano Energy*, 2018, **53**, 492–500.

7 X. Yu, Z. Yu, X. Zhang, Y. Zheng, Y. Duan, Q. Gao, R. Wu, B. Sun, M. Gao, G. Wang and S. Yu, *J. Am. Chem. Soc.*, 2019, **141**, 7537-7543.

8 H. Liu, R. Xie, Y. Luo, Z. Cui, Q. Yu, Z. Gao, Z. Zhang, F. Yang, X. Kang, S. Ge, S. Li, X. Gao, G. Chai, L. Liu and B. Liu, *Nat. Commun.*, 2022, **13**, 6382.

9 Y. Chen, G. Yu, W. Chen, Y. Liu, G. Li, P. Zhu, Q. Tao, Q. Li, J. Liu, X. Shen, H. Li, X. Huang, D. Wang, T. Asefa and X. Zou, *J. Am. Chem. Soc.*, 2017, **139**, 12370-12373.

10 H. Yang, Z. Chen, P. Guo, B. Fei and R. Wu, *Appl. Catal. B Environ.*, 2020, **261**, 118240.

11 C. Zhang, Y. Luo, J. Tan, Q. Yu, F. Yang, Z. Zhang, L. Yang, H. Cheng and B. Liu, *Nat. Commun.*, 2020, **11**, 3724.